Beyond the Woodward-Hoffman rules: what controls reactivity in eliminative aromatic ring-forming reactions?

A. D. Dinga Wonanke and Deborah L. Crittenden[*]

Department of Chemistry, University of Canterbury, Christchurch, New Zealand

E-mail: deborah.crittenden@canterbury.ac.nz

Abstract

The Mallory (photocyclization) and Scholl (thermal cyclohydrogenation) reactions are widely used in the synthesis of extended conjugated π systems of high scientific interest and technological importance, including molecular wires, semiconducting polymers and nanographenes. While simple electrocyclization reactions obey the Woodward-Hoffman rules, no such simple, general and powerful model is available for eliminative cyclization reactions due to their increased mechanistic complexity. In this work, detailed mechanistic investigations of prototypical reactions reveal that there is no single rate-determining step for thermal oxidative dehydrogenation reactions, but they are very sensitive to the presence and distribution of heteroatoms around the photocyclizing ring system. Key aspects of reactivity are correlated to the constituent ring oxidation potentials. For photocyclization reactions, planarization occurs readily and/or spontaneously following photo-excitation, and is promoted by heteroatoms within 5-membered ring adjacent to the photocyclizing site. Oxidative photocyclization requires intersystem crossing to proceed to products, while reactants configured to undergo purely eliminative photocyclization

---
[*]To whom correspondence should be addressed

could proceed to products entirely in the excited state. Overall, oxidative photocyclization seems to strike the optimal balance between synthetic convenience (ease of preparation of reactants, mild conditions, tolerant to chemical diversity in reactants) and favourable kinetic and thermodynamic properties.

Introduction

It has long been recognised that the most powerful insights into the nature of the physical world come when theory and experiment are unified:

"Experiment without theory is blind, but theory without experiment is mere intellectual play" – Immanuel Kant (1724-1804)

This special issue of *The Australian Journal of Chemistry* is dedicated to celebrating the career and 80th birthday of Emeritus Professor Graham Chandler, whose work has focussed on directly connecting theory and experiment,[1–15] and developing new ways of conceptualizing and rationalizing the behaviour of electrons within molecules and materials.[16–24]

Following in these footsteps, we seek to elucidate and understand the factors that control reactivity in a synthetically important class of aromatic-ring forming reactions; those that involve both intramolecular cyclization and elimination processes.[25]
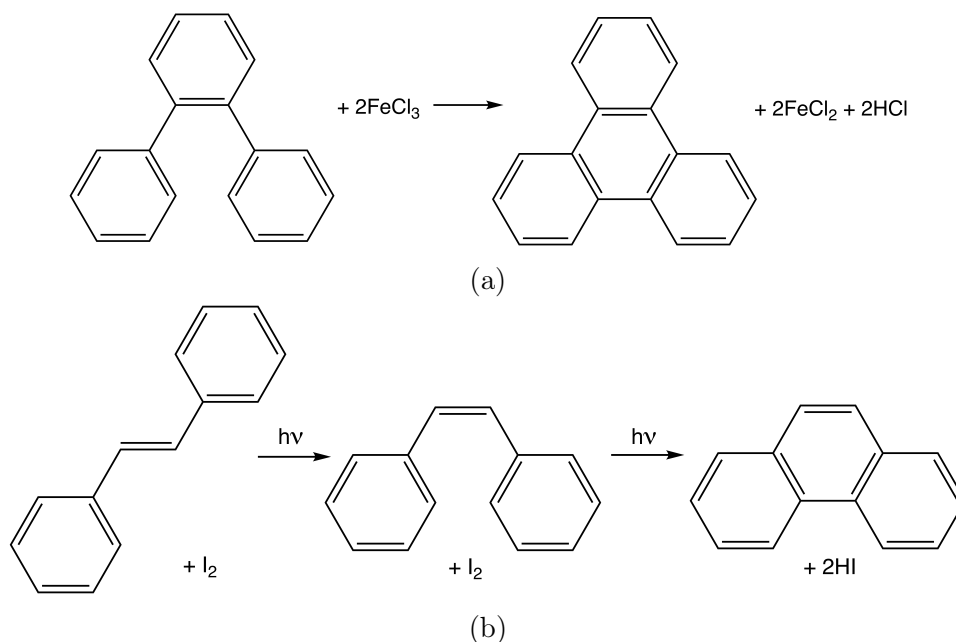

Figure 1: Balanced equations for prototypical (a) thermal [Scholl] and (b) photochemical [Mallory] oxidative cyclodehydrogenation reactions

For example, the Scholl reaction[26–29] (Figure 1(a)) is a thermal oxidative cyclodehydrogenation process that is used in the synthesis of atomically-precise nanomaterials with

3

useful electronic properties such as polythiophene semiconducting polymers,[30,31] polypyr-role conducting polymers[32,33] and very large polyaromatic hydrocarbons that are often referred to as nano-graphenes.[25,34,35]

Mallory reactions,[36–41] on the other hand, are photo-activated cyclization processes whose elimination step may be either oxidative (Figure 1(b)) or purely eliminative. They may be used to access a wider range of products from a wider range of readily accessible starting materials than the Scholl reaction. In particular, they do not need to be pre-aligned for ring formation, but can form the unconnected ring structure via trans-cis isomerization and/or bond rotation. The cyclizing centres may be heteroatoms and/or may have non-hydrogenic leaving groups attached. Mallory reactions are also more toler-ant to functional group substitution than Scholl reactions. However, the photoexcitation process can be reversible, or lead to alternative photoproducts, which can result in lower yields.[42–44]

The most likely proposed mechanisms for the Scholl[25,45–47] and Mallory[42,44,48] reactions are illustrated in Figures 2 and 3, and key similarities and differences between them are summarized in Table 1.

Table 1: Key steps in Mallory and Scholl cyclization processes, highlighting the similari-ties and differences between them.

	Mallory	Scholl
Mechanism	Photoexcite ↓ Cyclize ↓ Oxidise and dehydrogenate/ Eliminate	Oxidize ↓ Cyclize ↓ Dehydrogenate with further oxidation

For Scholl reactions and oxidative Mallory reactions, cyclization is initiated by mov-ing electrons either electrochemically to another molecule, or photochemically to another electronic state, and the dehydrogenation step is electrochemically driven. However, redox coupling is not required for the Mallory process to proceed through the purely
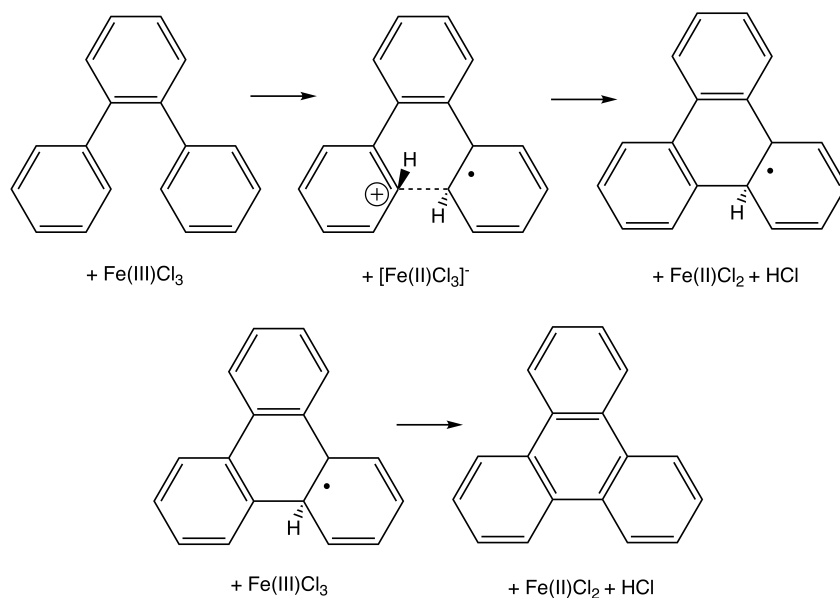
Figure 2: Thermal cyclization (Scholl reaction) proceeds via oxidative photocyclization and elimination (top), followed by a second oxidative elimination step (bottom)
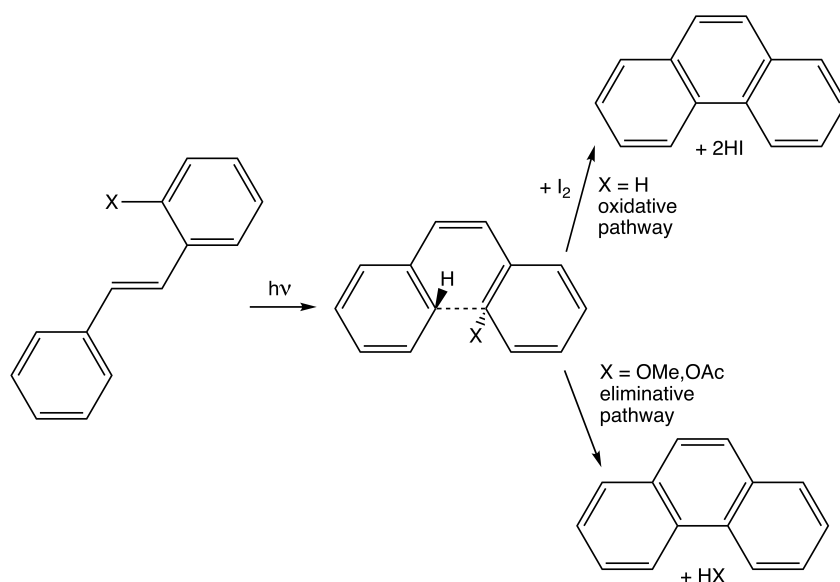

Figure 3: Mallory reaction mechanism: trans-cis isomerization and cyclization occur in first step, followed by either oxidative dehydrogenation (if oxidant present) or elimination (if reactant contains appropriately positioned leaving group)

5

eliminative pathway.

Although the general mechanisms illustrated in Figures 2 and 3 are reasonably well-supported by experimental and computational evidence,[25,42,44–48] they fall well short of providing the level of detail that is useful for synthetic chemists; given a reactant and set of reaction conditions, will a product form? Which set of reaction conditions should be tried first, if multiple reaction pathways are possible?

The Woodward-Hoffmann rules,[49–51] provide a simple, general and powerful model to answer questions of this nature for electrocyclization reactions, which are a much simpler class of cyclization reaction that are atom-economical and involve only concerted electron-transfer processes. The Woodward-Hoffmann rules were later generalized by Baldwin to describe a wider range of electrocyclization reactions involving heteroatoms and unusual ring features,[52,53] and map onto modern quantum chemical calculations through conceptual DFT.[54] However, all of these approaches lack information about the dehydrogenation/elimination process, so cannot be applied to the mechanistically more complex Scholl and Mallory reactions.

To address this deficiency, Laarhoven developed reactivity predictors for all-hydrocarbon photocyclization reactions based upon bond order analysis within Hückel molecular orbital theory.[55–58] The physical rationale behind this approach is that the number and/or strength of the existing π bonds at the cyclizing centres should decrease upon photo-excitation, facilitating the formation of a new intramolecular σ bond. Unfortunately, Laarhoven's rules turn out to be neither robust, nor generalizable, nor powerful, nor simple. They cannot be easily applied to molecules containing heteroatoms, do not apply at all to Scholl reactions, contain no information about reaction conditions or geometrical structure, and can fail to predict reaction outcomes correctly even where applicable.

Our aim here is to perform detailed mechanistic studies of both Mallory and Scholl reactions, to determine the key steric and electronic factors that control reactivity, with a view to developing simple, powerful, general and unified reactivity predictors for these

synthetically important classes of aromatic ring-forming reactions. We will focus particularly on structural modifications whose impact on reactivity is poorly explained by existing reactivity models; inclusion of heteroatoms and varying ring sizes within the photocyclizing ring system. Aromatic substituent effects on elimination reactions are already well understood[59,60] so will not be investigated in further detail here.

Methods

All reactants have the same basic framework structure (Figure 4) with varying rings, as illustrated in Table 2.
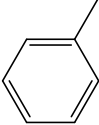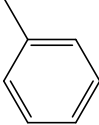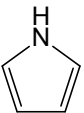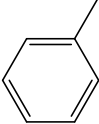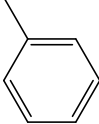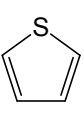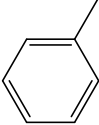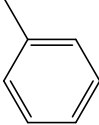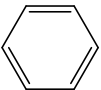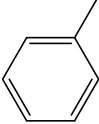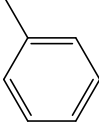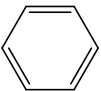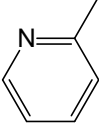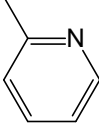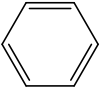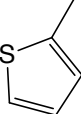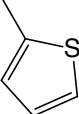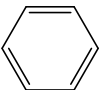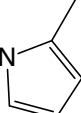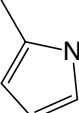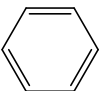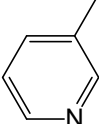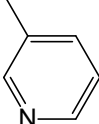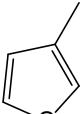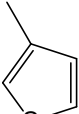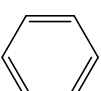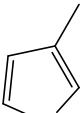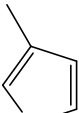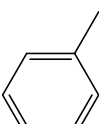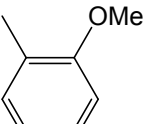

Figure 4: Framework structure for all reactants (left) and products (right) within our data set of molecules that undergo eliminative cyclization.

Reaction pathways are mapped out at B3LYP[61] using a 6-31G(d,p) basis[62] for all atoms except Cl^- (6-31+G(d))[63,64] and Fe (LanL2DZ).[65] Vertical excitation energies are computed at TD-B3LYP[66] with the same atomic orbital basis. Gibbs free energies are computed from ground and excited state electronic energies, ground state harmonic frequencies, moments of inertia and molecular masses using standard statistical thermodynamics formulae, discarding the imaginary frequency of each transition state. Solvation corrections to the free energy are computed using the conductor-like continuum solvation model[67] with a dielectric constant of 8.93 chosen to resemble dichloromethane. Complete details of all species involved in each reaction pathway are provided as Supporting Information.

All *ab initio* and statistical thermodynamics calculations are performed using QChem4.2.[68]

Table 2: IUPAC names and schematic representation of all molecules in our data set

IUPAC name	R$_1$	R$_2$	R$_3$
cis-1,2-diphenylethylene			
3,4-diphenylpyrrole			
3,4-diphenylthiophene			
1,2-diphenylbenzene			
2,2'-(1,2-phenylene)dipyridine			
2,2'-(1,2-phenylene)dithiophene			
2,2'-(1,2-phenylene)dipyrrole			
3,3'-(1,2-phenylene)dipyridine			
3,3'-(1,2-phenylene)dithiophene			
3,3'-(1,2-phenylene)dipyrrole			
1-(2-methoxyphenyl)-2-phenylbenzene			

Results and Discussion

Thermal cyclization

A prototypical reaction coordinate diagram for the radical cation mediated thermal oxidative cyclodehydrogenation of 1,2-diphenylbenzene is illustrated in Figure 5, and key thermodynamic parameters for all structural variants reported in Table 3.
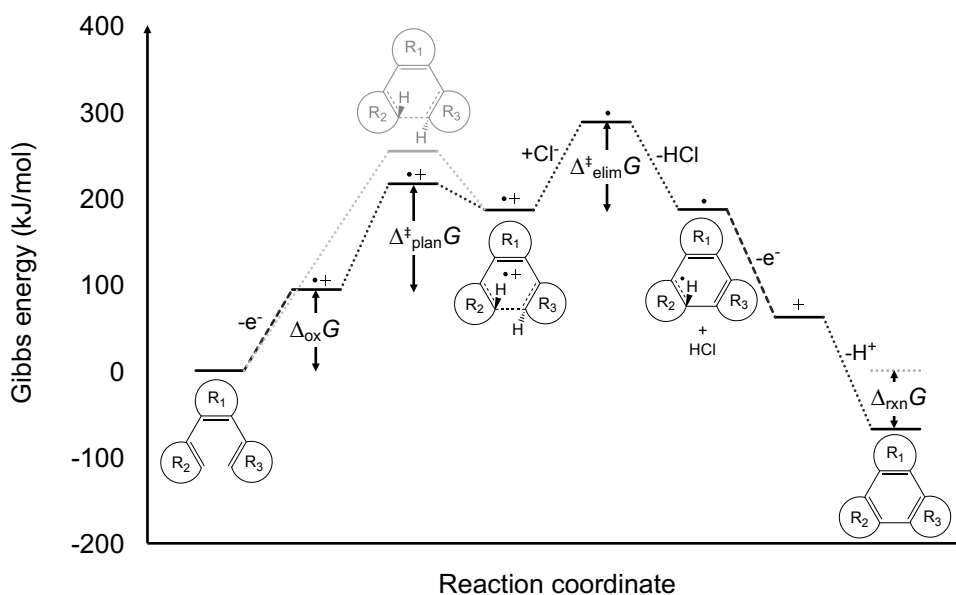
Figure 5: Reaction coordinate diagram for the thermal oxidative dehydrogenation of 1,2-diphenylbenzene (R_1 = benzene, R_2 = R_3 = phenyl), proceeding via the radical cation mechanism. The greyed-out lines represent the energy required for the planarization step of the reaction to proceed in a single step, in the absence of a strong oxidising agent.

On the whole, the data presented in Table 3 are consistent with experimental observations reported in the literature;[30–33,69,70] oxidative cyclodehydrogenation for all heteroaromatic molecules under investigation – except the dipyridine derivatives, for which no experimental data is available – occurs in the presence of strong oxidizing agents at room temperature. The substantial negative $\Delta_{\mathrm{rxn}}G$ values provide a strong thermodynamic driving force. The Gibbs energies of activation indicate that each reaction step, except the planarization of 3,4-diphenylpyrrole, should be thermally accessible at room temperature, assuming each molecule possesses $\frac{3N_{\mathrm{atom}}}{2}RT$ J/mol thermal energy (≈ 120 kJ/mol at 298.15 K). Although it is unlikely that all the available thermal energy would be chan-

9

¹²² neled into the reaction coordinate, it is also likely that we have overestimated barrier

¹²³ heights, as the continuum solvation model we have used does not account for explicit sol-

¹²⁴ vent stabilization of the radical cation intermediates, which is likely to have a significant

¹²⁵ stabilizing effect.[71,72] Finally, we note that the intrinsic accuracy of B3LYP for modelling

¹²⁶ isomerization reactions,[73] reaction enthalpies[74,75] and activation energies[74,75] lies in the

¹²⁷ $6 - 10$ kJ/mol range.

Table 3: Key thermodynamic quantities controlling the thermodynamic stability (Gibbs energy of reaction, $\Delta_{\mathrm{rxn}}G$) and kinetic reactivity (Gibbs energy of oxidation, $\Delta_{\mathrm{ox}}G$ and Gibbs energies of activation, $\Delta_{\mathrm{plan}}^{\ddagger}G$ and $\Delta_{\mathrm{elim}}^{\ddagger}G$) of candidate molecules for thermal oxidative cyclodehydrogenation (Scholl reaction).

| | | Both | Scholl | | | -oxidant |
R_1	$R_2 = R_3$	$\Delta_{\mathrm{rxn}}G$ (kJ/mol)	$\Delta_{\mathrm{ox}}G$ (kJ/mol)	$\Delta_{\mathrm{plan}}^{\ddagger}G$ (kJ/mol)	$\Delta_{\mathrm{elim}}^{\ddagger}G$ (kJ/mol)	$\Delta_{\mathrm{plan}}^{\ddagger}G$ (kJ/mol)
pyrrole	phenyl	-54.5	56.1	136.6	99.4	291.2
thiophene	phenyl	-55.0	98.8	93.9	73.0	307.2
benzene	phenyl	-67.7	93.9	122.5	101.9	254.1
benzene	2-pyridine	-71.8	118.3	103.5	73.0	246.4
benzene	2-thiophene	-97.7	60.0	98.2	106.4	264.2
benzene	2-pyrrole	-87.9	1.7	105.1	121.3	194.8
benzene	3-pyridine	-71.8	117.7	89.1	58.4	240.9
benzene	3-thiophene	-93.3	68.8	37.6	115.8	187.3
benzene	3-pyrrole	-90.8	6.5	46.1	118.9	172.4

¹²⁸ To the best of our knowledge, the only previous studies of oxidative cyclodehydrogenation

¹²⁹ reactions have either been performed entirely in the gas phase[46] or largely focussed on

¹³⁰ the arenium cation mechanism[76] that has since been experimentally shown[47] to be less

¹³¹ plausible than the radical cation mechanism investigated here. However, they do report

¹³² solvation-corrected $\Delta_{\mathrm{plan}}^{\ddagger}G$ values for 1,2-diphenylbenzene of 114.2 kJ/mol at B3LYP/6-

¹³³ 31G* and 105.9 kJ/mol at BHandHLYP/6-31G* that agree reasonably with the 122.5

¹³⁴ kJ/mol reported here.

¹³⁵ High-level gas phase CASPT2/6-31G* calculations on the initial planarization step of the

¹³⁶ 2,2'-(1,2-phenylene)dithiophene and 3,3'-(1,2-phenylene)dithiophene reactions have been

¹³⁷ computed in the absence of oxidant, in the context of modelling the factors that control

¹³⁸ photoswitchability of these molecules.[77] In principle, their reported gas phase values are

not directly comparable to our solvation-corrected values. However, the polarity of the molecule does not change substantially upon planarization in the absence of oxidant, so the corresponding solvation free energy change is also small, according to the continuum solvation model we use (full details accessible in Supporting Information). Therefore, the difference between their reported values of 236.0 kJ/mol and 193.3 kJ/mol, respectively, and ours of 264.2 kJ/mol and 187.3 kJ/mol, are largely due to differences in electronic structure models.

Overall, our model qualitatively and semi-quantitatively reproduces existing experimental and computational data, so can be confidently used to identify trends in reactivity due to inclusion of heteroatoms and variation of ring sizes within the cyclizing ring system.

From Table 3, it is clear that the Gibbs energy of oxidation, $\Delta_{ox}G$, is most strongly influenced by the identity of the terminal rings, but not the position of the heteroatom within the cyclizing ring system. Pyridine increases the barrier to oxidation relative to benzene, thiophene decreases it, and pyrrole substantially decreases it. As expected, these trends are roughly correlated with the oxidation potentials of each ring substituent drawn from the literature[78,79] and reported in Table 4

Table 4: Oxidation potentials of ring substituents, measured under the same experimental conditions[79]

Molecule	E_{ox} (V)
benzene	2.08
pyridine	1.82
thiophene	1.60
pyrrole	0.76

Gibbs energies of activation for planarization, $\Delta^{\ddagger}_{plan}G$, are substantially decreased by having a heteroatom adjacent to the photocyclizing site, and slightly decreased by the presence of a thiophene ring anywhere within the cyclizing system. This suggests that the primary determinant of the barrier to oxidative cyclization is the ability to alleviate ring strain.

Gibbs energies of activation for elimination, $\Delta^{\ddagger}_{\text{elim}}G$ obey similar trends to those of oxidation, only in the opposite direction. For molecules with terminal ring substituents, pyrrole and thiophene both raise the barrier while pyridine substantially decreases it. Substitution of the central ring by pyrrole has little effect while thiophene substituent lowers the barrier for reasons that are not entirely clear to us.

Taking all of the above competing effects into account, the molecule with lowest overall rate-determining free energy barrier is 3,4-diphenylthiophene.

Oxidative photocyclization

A prototypical reaction coordinate diagram for the oxidative photocyclization of 1,2-diphenylbenzene is illustrated in Figure 6, and key thermodynamic parameters for all structural variants reported in Table 5.
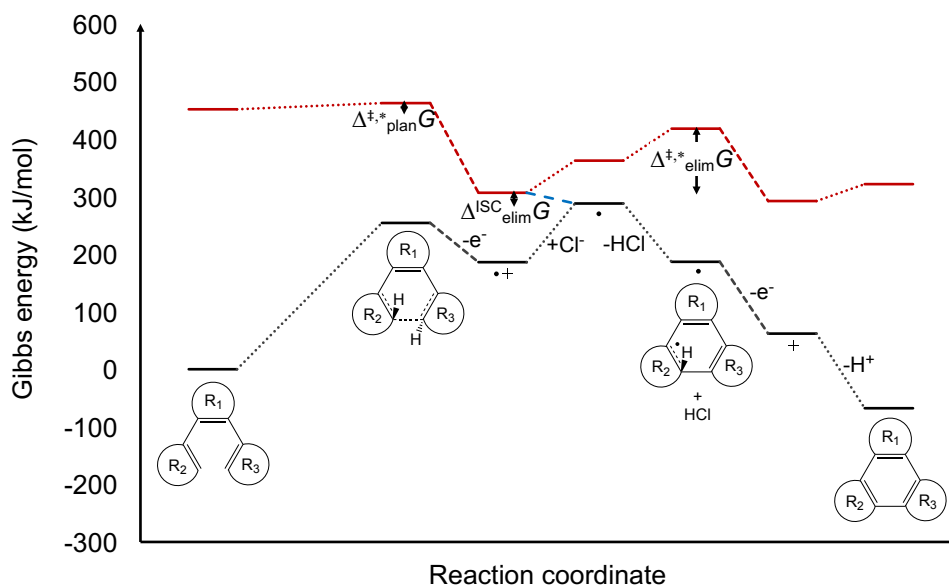
Figure 6: Ground (black) and excited state (red) reaction coordinate diagrams for the photochemical oxidative dehydrogenation of 1,2-diphenylbenzene (R_1 = benzene, R_2 = R_3 = phenyl), with intersystem crossing proposed to occur during the first step of the elimination process, as indicated in blue.

As far as we are aware, there are no prior mechanistic studies covering all stages of the oxidative Mallory photocyclization process. However, the first step in the photocy-

Table 5: Key thermodynamic quantities controlling the thermodynamic stability (Gibbs energy of intersystem crossing, $\Delta_{\mathrm{elim}}^{\mathrm{ISC}}G$) and kinetic reactivity (excited state Gibbs energies of activation, $\Delta_{\mathrm{plan}}^{\ddagger,*}G$ and $\Delta_{\mathrm{elim}}^{\ddagger,*}G$) of candidate molecules for photochemical oxidative cyclodehydrogenation (Mallory reaction). Gibbs energies of reaction are the same as for the Scholl reaction, as reported in Table 3.

| R$_1$ | R$_2$ = R$_3$ | Mallory | | |
		$\Delta_{\mathrm{plan}}^{\ddagger,*}G$ (kJ/mol)	$\Delta_{\mathrm{elim}}^{\ddagger,*}G$ (kJ/mol)	$\Delta_{\mathrm{elim}}^{\mathrm{ISC}}G$ (kJ/mol)
ethene	phenyl	19.2	85.2	-52.8
pyrrole	phenyl	14.9	148.3	-11.6
thiophene	phenyl	17.8	123.1	-26.6
benzene	phenyl	10.7	111.3	-18.6
benzene	2-pyridine	8.8	105.3	-28.0
benzene	2-thiophene	36.8	92.7	-69.3
benzene	2-pyrrole	32.6	155.3	-44.9
benzene	3-pyridine	6.0	117.3	-31.9
benzene	3-thiophene	-73.1	155.3	-39.1
benzene	3-pyrrole	-20.7	214.3	-31.7

173 clization of 2,2'-(1,2-phenylene)dithiophene and 3,3'-(1,2-phenylene)dithiophene has been

174 extensively investigated[48,77] in light of their potential utility as molecular photoswitches.

175 Although our vertical excitation energies are not directly comparable with the adiabatic

176 values reported in the literature,[77] our results are nonetheless consistent with previous

177 findings that planarization proceeds spontaneously in the first excited state for 3,3'-(1,2-

178 phenylene)dithiophene, and partial planarization proceeds spontaneously for 2,2'-(1,2-

179 phenylene)dithiophene.

180 Overall, the $\Delta_{\mathrm{plan}}^{\ddagger,*}G$ values presented in Table 5 imply that planarization proceeds either

181 readily (low positive values) or spontaneously (negative values) following photo-excitation

182 for all molecules in our data set. Planarization appears to be strongly enhanced by the

183 presence of a heteroatom adjacent to the photocyclizing centre, but retarded by distant

184 heteroatoms within 5-membered rings, or the presence of an ethylene bridge within the

185 molecule.

186 By analogy with the Scholl mechanism data presented in the previous section, a number

187 of these reactions could proceed thermally in the excited state, with $\Delta_{\mathrm{elim}}^{\ddagger,*}G$ values < 120

kJ/mol. However, it is far more likely that they undergo a thermodynamically favourable intersystem crossing ($\Delta_{\mathrm{elim}}^{\mathrm{ISC}}G < 0$), mediated by vibronic interactions with the oxidant.

Comparing the data presented in Tables 3 and 5, it appears that photo-mediated oxidative cyclodehydrogenation reactions will occur more readily and under milder conditions than their thermal counterparts, with free energy barriers that are less sensitive to the identity of the reactants.

Eliminative photocyclization

Finally, it remains to compare the oxidative and purely eliminative photocyclization processes illustrated in Figure 7. Synthetically, the oxidative route is easier, as it does not require appropriate leaving groups to be pre-attached to the photocyclizing rings in appropriate positions, although the eliminative route has a shorter work-up as the low molecular weight elimination product can simply be distilled off from the reaction mixture.
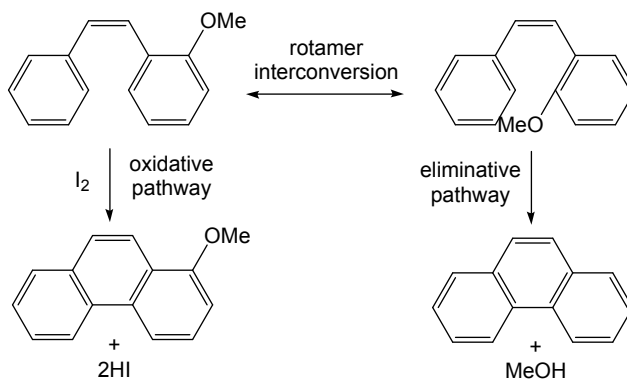
Figure 7: Oxidative (left) and eliminative (right) photocyclization pathways

Reaction coordinate diagrams for 1-(2-methoxyphenyl)-2-phenylbenzene, a prototypical molecule that can undergo both oxidative and eliminative photocyclization, are illustrated in Figure 8. Key thermodynamic parameters for both pathways are reported in Table 5, along with 1,2-diphenylbenzene reference data.

In contrast to the unsubstituted parent molecule 1,2-diphenylbenzene, 1-(2-methoxyphenyl)-2-phenylbenzene has an unfavourable intersystem crossing free energy along the oxidative
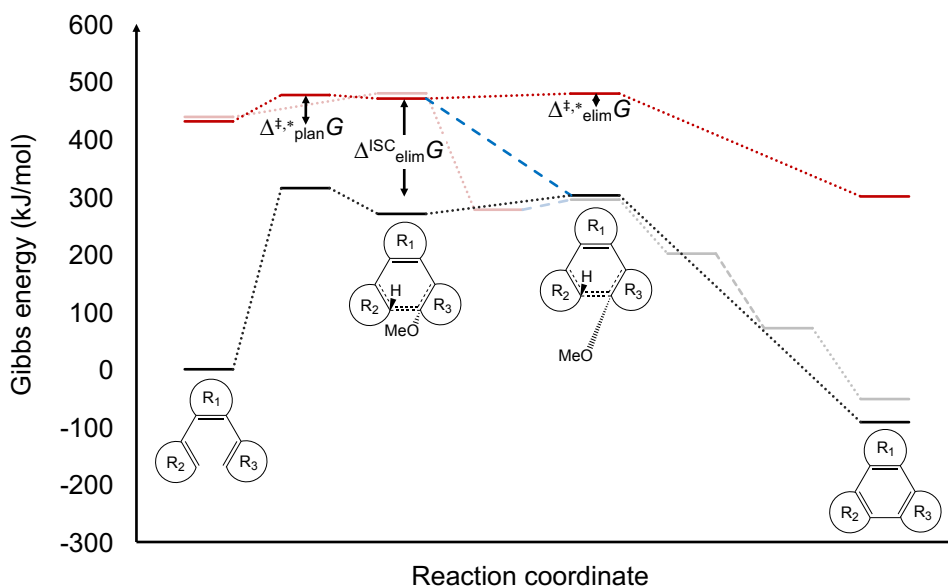
Figure 8: Ground (black) and excited state (red) reaction coordinate diagrams for the photochemical eliminative cyclization of 1-(2-methoxyphenyl)-2-phenylbenzene (R_1 = benzene, R_2 = phenyl, R_3 = 2-methoxyphenyl). For reference, the proposed oxidative pathway is shown greyed-out.

Table 6: Gibbs energies of reaction ($\Delta_{\mathrm{rxn}}G$), Gibbs energies of activation ($\Delta_{\mathrm{plan}}^{\ddagger,*}G$, $\Delta_{\mathrm{elim}}^{\ddagger,*}G$) and Gibbs energies of intersystem crossing ($\Delta_{\mathrm{elim}}^{\mathrm{ISC}}G$) capturing key characteristics of the potential energy surfaces for oxidative and purely eliminative photocyclization of 1-(2-methoxyphenyl)-2-phenylbenzene (R_1 = benzene, R_2 = phenyl, R_3 = 2-methoxyphenyl).

Molecule	Pathway	$\Delta_{\mathrm{rxn}}G$ (kJ/mol)	$\Delta_{\mathrm{plan}}^{\ddagger,*}G$ (kJ/mol)	$\Delta_{\mathrm{elim}}^{\ddagger,*}G$ (kJ/mol)	$\Delta_{\mathrm{elim}}^{\mathrm{ISC}}G$ (kJ/mol)
1,2-diphenylbenzene	oxidative	-67.7	10.7	111.3	-18.6
1-(2-methoxyphenyl)-2-phenylbenzene	oxidative	-51.7	41.0	154.6	17.5
1-(2-methoxyphenyl)-2-phenylbenzene	eliminative	-91.8	45.8	8.7	-168.1

pathway, higher free energy of planarization and lower overall thermodynamic stability of the products, i.e. it is disfavoured over the unsubstituted molecule in every respect. Therefore, adding on a methoxy leaving group is a poor synthetic strategy unless the eliminative pathway is strongly favourable.

The eliminative pathway has a low energy barrier for progression from the planar intermediate to the excited state product and the intersystem crossing along this pathway is strongly exergonic, suggesting that the reaction could proceed via either pathway. However, as there is no obvious mechanism for the intersystem crossing to occur, we hypothesise that this reaction proceeds to completion in the excited state.

Finally, we note that the free energies of activation for planarization, $\Delta^{\ddagger,*}_{\mathrm{plan}}G$, are the largest of all reactants considered in this study, regardless of which rotamer is involved and which pathway is being followed.

Conclusions

Oxidative Mallory reactions appear to optimally balance synthetic convenience (ease of preparation of reactants, mild conditions, tolerant to chemical diversity in reactants) against favourable kinetic and thermodynamic properties. Thermal oxidative cyclodehydrogenation (Scholl) reactions are far more sensitive to the nature of the rings comprising the reactant molecules, which can have both disadvantages (capricious reactivity) and advantages (controllability). There does not seem to be any additional advantage pursuing eliminative photocyclization over oxidative, from the limited results presented here. Future work should further investigate the interplay between substituent effects, ring strain and heteroatom effects.

Supporting Information Available

Molecular coordinates and raw *ab initio* data for all species involved in each reaction pathway are included as Supporting Information.

16

Conflict of Interest

The authors declare no conflicts of interest.

Acknowledgement

References

(1) Chandler, G. S.; Wajrak, M.; Khan, R. N. Neutron diffraction structures of water in crystalline hydrates of metal salts. *Acta. Cryst. B* **2015**, *71*, 275–284.

(2) Talbi, D.; Chandler, G. S. Theoretical infrared spectra of biphenyl, terphenyls and tetraphenyls for astrophysical purposes. *J. Mol. Spec.* **2012**, *275*, 21–27.

(3) Fuller, R. O.; Chandler, G. S.; Davis, J. R.; McKinley, A. J. Matrix isolation ESR and theoretical studies of metal phosphides. *J. Chem. Phys.* **2010**, *133*, 164311.

(4) Bytheway, I.; Grimwood, D. J.; Figgis, B. N.; Chandler, G. S.; Jayatilaka, D. Wavefunctions derived from experiment. IV. Investigation of the crystal environment of ammonia. *Acta Cryst. A* **2002**, *58*, 244–251.

(5) Li, Z. C.; Jayatilaka, D.; Figgis, B. N.; Chandler, G. S. A theoretical study of the polarized neutron scattering from Cs_3CoCl_5. *J. Chem. Phys.* **2001**, *114*, 2687–2697.

(6) Chandler, G. S.; Figgis, B. N.; Li, Z. C. Ab initio calculation of experimental structure factors for $Ni(NH_3)_4(NO_2)_2$. *Phys. Chem. Chem. Phys.* **2000**, *2*, 3743–3751.

(7) Chandler, G. S.; Jayatilaka, D.; Wolff, S. K. Electronic structure from polarised neutron diffraction. *Aust. J. Phys.* **1996**, *49*, 261–272.

(8) Wolff, S. K.; Jayatilaka, D.; Chandler, G. S. An ab-initio calculation of magnetic structure factors for Cs_3COCl_5 including spin-orbit and finite magnetic-field effects. *J. Chem. Phys.* **1995**, *103*, 4562–4571.

(9) Chandler, G. S.; Figgis, B. N.; Reynolds, P. A.; Wolff, S. K. Ab initio theoretical calculation of experimental structure factors for $(ND_4)_2Cu(SO_4)_2.6D_2O$ at 9 K. *Chem. Phys. Lett.* **1994**, *225*, 421–426.

(10) McLean, A. D.; Liu, B.; Chandler, G. S. Computed self-consistent field and singles and doubles configuration-interaction spectroscopic data and dissociation-energies for the diatomics B_2, C_2, N_2, O_2, F_2, CN, CP, CS, PN, SiC, SiN, SiO, SiP and their ions. *J. Chem. Phys.* **1992**, *97*, 8459–8464.

(11) Chandler, G. S.; Christos, G. A.; Figgis, B. N.; Reynolds, P. A. Calculation of spin and charge-densities in hexaaqua transition-metal(II) ions and their comparison with experiment. *J. Chem. Soc. - Faraday Trans.* **1992**, *88*, 1961–1969.

(12) Chandler, G. S.; Deeth, R. J.; FIggis, B. N.; Phillips, R. A. Theoretical versus experimental charge and spin-density distributions in trans–[Ni(NH$_3$)$_4$(NO$_2$)$_2$]. *J. Chem. Soc. - Dalton Trans.* **1990**, 1417–1427.

(13) Barnes, L. A.; Chandler, G. S.; Figgis, B. N. Orbital magnetization in CoCl$_4^{2-}$ and Co(phthalocyanine) from polarized neutron-diffraction. *Mol. Phys.* **1989**, *68*, 711–735.

(14) Barnes, L. A.; Glass, R.; Reynolds, P. A.; Figgis, B. N.; Chandler, G. S. The effect of configuration-interaction on atomic scattering factors for transition-metals. *Acta Cryst. A* **1984**, *40*, 620–624.

(15) Chandler, G. S.; Figgis, B. N.; Phillips, R. A.; Reynolds, P. A.; Mason, R.; Williams, G. A. Spin-density and bonding in the CoCl$_4^{2-}$ ion in CS$_3$COCl$_5$. The comparison of theory and experiment. *Proc. Royal Soc. London A* **1982**, *384*, 31–48.

(16) Gould, M. D.; Taylor, C.; Wolff, S. K.; Chandler, G. S.; Jayatilaka, D. A definition for the covalent and ionic bond index in a molecule. *Theor. Chem. Acc.* **2008**, *119*, 275–290.

(17) Bytheway, I.; Chandler, G. S.; Figgis, B. N. Can a multipole analysis faithfully reproduce topological descriptors of a total charge density? *Acta. Cryst. A* **2002**, *58*, 451–459.

(18) Jayatilaka, D.; Chandler, G. S. Spatial symmetry and equivalence with unrestricted Hartree-Fock wavefunctions: application to the prediction of spin densities. *Mol. Phys.* **1997**, *92*, 471–476.

(19) Cassam-Chenai, P.; Chandler, G. S. Spin-unrestricted calculations in quantum chemistry. *Int. J. Quantum. Chem.* **1993**, *46*, 593–607.

(20) Gould, M. D.; Chandler, G. S. Bases for the irreducible representations of O(3) symmetry adapted to a crystallographic point group. *Int. J. Quant. Chem.* **1987**, *31*, 535–563.

(21) Chandler, G. S.; Glass, R. The calculation of atomic polarizabilities with emphasis on the 1st transition series. *Int. Rev. Phys. Chem.* **1986**, *5*, 293–300.

(22) Barnes, L. A.; Chandler, G. S.; Figgis, B. N.; Khan, D. C. A program to calculate magnetic form-factors for transition-metal systems. *Comp. Phys. Comm.* **1985**, *36*, 373–382.

(23) Chandler, G. S.; Spackman, M. A. Pseudo-atom expansions of the 1st-row diatomic hydride electron-densities. *Acta Cryst. A* **1982**, *38*, 225–239.

(24) Chandler, G. S.; Spackman, M. A.; Varghese, J. N. Pseudo-atom expansions of the H_2 electron-density. *Acta Cryst. A* **1980**, *36*, 657–669.

(25) Kivala, M.; Wu, D.; Feng, X.; Li, C.; Müllen, K. Cyclodehydrogenation in the synthesis of graphene-type molecules. *Mat. Sci. Tech.* **2012**,

(26) Scholl, R.; Seer, C. Abspaltung aromatisch gebundenen Wasserstoffs und Verknüpfung aromatischer Kerne durch Aluminiumchlorid. *Eur. J. Org. Chem.* **1912**, *394*, 111–177.

(27) Scholl, R.; Seer, C. Über die Abspaltung aromatisch gebundenen Wasserstoffs unter Verknüpfung aromatischer Kerne durch Aluminiumchlorid. *Eur. J. Inorg. Chem.* **1922**, *55*, 109–117.

(28) Kovacic, P.; Wu, C. Reaction of ferric chloride with benzene. *J. Polymer Sci. A* **1960**, *47*, 45–54.

(29) Kovacic, P.; Wu, C.; Stewart, R. W. Reaction of ferric chloride with alkylbenzenes. *J. Am. Chem. Soc.* **1960**, *82*, 1917–1923.

20

(30) Grimsdale, A. C.; Leok Chan, K.; Martin, R. E.; Jokisz, P. G.; Holmes, A. B. Synthesis of light-emitting conjugated polymers for applications in electroluminescent devices. *Chem. Rev.* **2009**, *109*, 897–1091.

(31) Rieger, R.; Beckmann, D.; Pisula, W.; Steffen, W.; Kastler, M.; Müllen, K. Rational Optimization of benzo [2, 1-b; 3, 4-b?] dithiophene-containing polymers for organic field-effect transistors. *Adv. Mat.* **2010**, *22*, 83–86.

(32) Bhattacharya, A.; De, A. Conducting composites of polypyrrole and polyaniline a review. *Prog. Solid State Chem.* **1996**, *24*, 141–181.

(33) Lu, Y. Q.; Shi, G. Q.; Li, C.; Liang, Y. Q. Thin polypyrrole films prepared by chemical oxidative polymerization. *J. Appl. Polym. Sci.* **1998**, *70*, 2169–2172.

(34) Geim, A. K.; Novoselov, K. S. The rise of graphene. *Nature Mat.* **2007**, *6*, 183–191.

(35) Wu, J.; Pisula, W.; Müllen, K. Graphenes as potential material for electronics. *Chem. Rev.* **2007**, *107*, 718–747.

(36) Mallory, F. B.; Gordon, J. T.; Wood, C. S.; Lindquist, L. C.; Savitz, M. L. Photochemistry of stilbenes .1. *J. Am. Chem. Soc.* **1962**, *84*, 4361–4362.

(37) Mallory, F. B.; Wood, C. S.; Gordon, J. T. Photochemistry of stilbenes .2. Substituent effects on rates of phenanthrene formation. *J. Am. Chem. Soc.* **1963**, *85*, 828–829.

(38) Mallory, F. B.; Wood, C. S.; Gordon, J. T. Photochemistry of stilbenes .3. Some aspects of mechanism of photocyclization to phenanthrenes. *J. Am. Chem. Soc.* **1964**, *86*, 3094–3102.

(39) Wood, C. S.; Mallory, F. B. Photochemistry of stilbenes .4. Preparation of substituted phenanthrenes. *J. Org. Chem.* **1964**, *29*, 3373–3377.

(40) Sudhakar, A.; Katz, T. J.; Yang, B. W. Synthesis of a helical metallocene oligomer. *J. Am. Chem. Soc.* **1986**, *108*, 2790–2791.

21

(41) Liu, L. B.; Yang, B. W.; Katz, T. J.; Poindexter, M. K. Improved methodology for photocyclization reactions. *J. Org. Chem.* **1991**, *56*, 3769–3775.

(42) Mallory, F. B.; Mallory, C. W. Photocyclization of stilbenes and related molecules. *Org. React.* **1984**, *30*, 1–456.

(43) Tominaga, Y.; Castle, R. N. Photocyclization of aryl- and heteroaryl-2-propenoic acid derivatives. Synthesis of polycyclic heterocycles. *J. Heterocyc. Chem.* **1996**, *33*, 523–538.

(44) Jorgensen, K. B. Photochemical oxidative cyclisation of stilbenes and stilbenoids - the Mallory reaction. *Molecules* **2010**, *15*, 4334–4358.

(45) Hammerich, O.; Parker, V. D. Kinetics and mechanisms of reactions of organic cation radicals in solution. *Advances in physical organic chemistry* **1984**, *20*, 55–189.

(46) Di Stefano, M.; Negri, F.; Carbone, P.; Müllen, K. Oxidative cyclodehydrogenation reaction for the design of extended 2D and 3D carbon nanostructures: A theoretical study. *Chem. Phys.* **2005**, *314*, 85–99.

(47) Zhai, L.; Shukla, R.; Wadumethrige, S. H.; Rathore, R. Probing the arenium-ion (proton transfer) versus the cation-radical (electron transfer) mechanism of Scholl reaction using DDQ as oxidant. *J. Org. Chem.* **2010**, *75*, 4748–4760.

(48) Guillaumont, D.; Kobayashi, T.; Kanda, K.; Miyasaka, H.; Uchida, K.; Kobatake, S.; Shibata, K.; Nakamura, S.; Irie, M. An ab initio MO study of the photochromic reaction of dithienylethenes. *J. Phys. Chem. A* **2002**, *106*, 7222–7227.

(49) Woodward, R. B.; Hoffmann, R. Stereochemistry of electrocyclic reactions. *J. Am. Chem. Soc.* **1965**, *87*, 395–397.

(50) Hoffmann, R.; Woodward, R. B. Selection rules for concerted cycloaddition reactions. *J. Am. Chem. Soc.* **1965**, *87*, 2046–2048.

(51) Woodward, R. B.; Hoffmann, R. The conservation of orbital symmetry. *Angewandte Chemie* **1969**, *8*, 781–853.

(52) Baldwin, J. E. Rules for ring-closure. *J. Chem. Soc. - Chem. Comm.* **1976**, 734–736.

(53) Gilmore, K.; Mohamed, R. K.; Alabugin, I. V. The Baldwin rules: revised and extended. *Wiley Interdisciplinary Reviews: Computational Molecular Science* **2016**, *6*, 487–514.

(54) Geerlings, P.; Ayers, P. W.; Toro-Labbe, A.; Chattaraj, P. K.; De Proft, F. The Woodward-Hoffmann rules reinterpreted by conceptual Density Functional Theory. *Acc. Chem. Res.* **2012**, *45*, 683–695.

(55) Laarhoven, W. H.; Cuppen, T. J. H.; Nivard, R. J. F. Photodehydrocyclizations in stilbene-like compounds. *Rec. Trav. Chim. - J. Roy. Neth. Chem.* **1968**, *87*, 687–698.

(56) Laarhoven, W. H.; Cuppen, T. J. H.; Nivard, R. J. F. Photodehydrocyclizations in stilbene-like compounds. 2. Photochemistry of distyrylbenzenes. *Tetrahedron* **1970**, *26*, 1069–1083.

(57) Laarhoven, W. H.; Cuppen, T. J. H.; Nivard, R. J. F. Photodehydrocyclizations in stilbene-like compounds. 3. Effect of steric factors. *Tetrahedron* **1970**, *26*, 4865–4881.

(58) Laarhoven, W. H. Photochemical cyclizations and intramolecular cyclo-additions of conjugated arylolefins .1. Photocyclization with dehydrogenation. *Rec. Trav. Chim. - J. Roy. Neth. Chem.* **1983**, *102*, 185–204.

(59) Stirling, C. J. M. Leaving groups and nucleofugality in elimination and other organic reactions. *Acc. Chem. Res.* **1979**, *12*, 198–203.

(60) King, B. T.; Kroulík, J.; Robertson, C. R.; Rempala, P.; Hilton, C. L.; Korinek, J. D.; Gortari, L. M. Controlling the Scholl reaction. *J. Org. Chem.* **2007**, *72*, 2279–2288.

(61) Becke, A. D. A new mixing of Hartree–Fock and local density-functional theories. *J. Chem. Phys.* **1993**, *98*, 1372–1377.

(62) Hehre, W. J.; Ditchfield, R.; Pople, J. A. Self-consistent molecular orbital methods. XII. Further extensions of gaussian-type basis sets for use in molecular orbital studies of organic molecules. *J. Chem. Phys.* **1972**, *56*, 2257–2261.

(63) Francl, M. M.; Pietro, W. J.; Hehre, W. J.; Binkley, J. S.; Gordon, M. S.; De-Frees, D. J.; Pople, J. A. Self-consistent molecular orbital methods. XXIII. A polarization-type basis set for second-row elements. *J. Chem. Phys.* **1982**, *77*, 3654–3665.

(64) Frisch, M. J.; Pople, J. A.; Binkley, J. S. Self-consistent molecular orbital methods 25. Supplementary functions for Gaussian basis sets. *J. Chem. Phys.* **1984**, *80*, 3265–3269.

(65) Hay, P. J.; Wadt, W. R. Ab initio effective core potentials for molecular calculations. Potentials for the transition metal atoms scandium to mercury. *J. Chem. Phys* **1985**, *82*, 270–283.

(66) Hirata, S.; Head-Gordon, M. Time-dependent density functional theory within the Tamm–Dancoff approximation. *Chem. Phys. Lett.* **1999**, *314*, 291–299.

(67) Barone, V.; Cossi, M. Quantum calculation of molecular energies and energy gradients in solution by a conductor solvent model. *J. Phys. Chem. A* **1998**, *102*, 1995–2001.

(68) Shao, Y.; Gan, Z.; Epifanovsky, E.; Gilbert, A. T.; Wormit, M.; Kussmann, J.; Lange, A. W.; Behn, A.; Deng, J.; Feng, X.; *et al*, Advances in molecular quantum chemistry contained in the Q-Chem 4 program package. *Molecular Physics* **2015**, *113*, 184–215.

(69) Kang, H. C.; Geckeler, K. E. Enhanced electrical conductivity of polypyrrole prepared by chemical oxidative polymerization: effect of the preparation technique and polymer additive. *Polymer* **2000**, *41*, 6931–6934.

(70) Stanke, D.; Hallensleben, M. L.; Toppare, L. Graft copolymers and composites of poly (methyl methacrylate) and polypyrrole Part I. *Synthetic metals* **1995**, *72*, 89–94.

(71) Kelly, C. P.; Cramer, C. J.; Truhlar, D. G. Adding explicit solvent molecules to continuum solvent calculations for the calculation of aqueous acid dissociation constants. *J. Phys. Chem. A* **2006**, *110*, 2493–2499.

(72) da Silva, E. F.; Svendsen, H. F.; Merz, K. M. Explicitly representing the solvation shell in continuum solvent calculations. *J. Phys. Chem. A* **2009**, *113*, 6404–6409.

(73) Tirado-Rives, J.; Jorgensen, W. L. Performance of B3LYP density functional methods for a large set of organic molecules. *J. Chem. Theor. Comp.* **2008**, *4*, 297–306.

(74) Ess, D. H.; Houk, K. Activation energies of pericyclic reactions: Performance of DFT, MP2, and CBS-QB3 methods for the prediction of activation barriers and reaction energetics of 1, 3-dipolar cycloadditions, and revised activation enthalpies for a standard set of hydrocarbon pericyclic reactions. *J. Phys. Chem. A* **2005**, *109*, 9542–9553.

(75) Guner, V.; Khuong, K. S.; Leach, A. G.; Lee, P. S.; Bartberger, M. D.; Houk, K. A standard set of pericyclic reactions of hydrocarbons for the benchmarking of computational methods: the performance of ab initio, density functional, CASSCF, CASPT2, and CBS-QB3 methods for the prediction of activation barriers, reaction energetics, and transition state geometries. *J. Phys. Chem. A* **2003**, *107*, 11445–11459.

(76) Rempala, P.; Kroulík, J.; King, B. T. Investigation of the mechanism of the intramolecular Scholl reaction of contiguous phenylbenzenes. *J. Org. Chem.* **2006**, *71*, 5067–5081.

(77) Perrier, A.; Aloise, S.; Olivucci, M.; Jacquemin, D. Inverse versus normal dithienylethenes: computational investigation of the photocyclization reaction. *J. Phys. Chem. Lett.* **2013**, *4*, 2190–2196.

25

(78) Weinberg, N.; Weinberg, H. Electrochemical oxidation of organic compounds. *Chemical Reviews* **1968**, *68*, 449–523.

(79) Loveland, J. W.; Dimeler, G. Anodic Voltammetry to+ 2.0 Volts. Application to Hydrocarbons and Oxidation Stability Studies. *Analytical Chemistry* **1961**, *33*, 1196–1201.